

## Amorphization/recrystallization of buried amorphous silicon layer induced by oxygen ion implantation

J. P. de Souza, C. A. Cima, P. F. P. Fichtner, and H. Boudinov

Citation: [Journal of Applied Physics](#) **95**, 877 (2004); doi: 10.1063/1.1636264

View online: <http://dx.doi.org/10.1063/1.1636264>

View Table of Contents: <http://scitation.aip.org/content/aip/journal/jap/95/3?ver=pdfcov>

Published by the [AIP Publishing](#)

---



## Re-register for Table of Content Alerts

Create a profile.



Sign up today!



# Amorphization/recrystallization of buried amorphous silicon layer induced by oxygen ion implantation

J. P. de Souza<sup>a)</sup>

*Instituto de Física, Universidade Federal do Rio Grande do Sul, 91501-970, Porto Alegre, RS, Brazil*

C. A. Cima<sup>b)</sup>

*DENELE, Fundação de Ciência e Tecnologia, 90010-460, Porto Alegre, RS, Brazil*

P. F. P. Fichtner

*Escola de Engenharia, Universidade Federal do Rio Grande do Sul, 90035-190, Porto Alegre, RS, Brazil*

H. Boudinov

*Instituto de Física, Universidade Federal do Rio Grande do Sul, 91501-970, Porto Alegre, RS, Brazil*

(Received 23 July 2003; accepted 30 October 2003)

In this paper we discuss the structural modifications observed in a buried amorphous Si (*a*-Si) layer containing high oxygen concentration level (up to  $\sim 3$  at. %) after being implanted at elevated temperature with  $^{16}\text{O}^+$  ions. For implants conducted at temperatures lower than  $150^\circ\text{C}$ , the *a*-Si layer expands via layer by layer amorphization at the front and back amorphous–crystalline (*a*–*c*) interfaces. When performed at temperatures above  $150^\circ\text{C}$ , the implants lead to the narrowing of the buried *a*-Si layer through ion beam-induced epitaxial crystallization at both *a*–*c* interfaces. Cross section transmission electron microscopy analysis of samples implanted at  $400^\circ\text{C}$  revealed an array of microtwins and a dislocation network band in the recrystallized material. In samples implanted at  $550^\circ\text{C}$ , only a buried dislocation network band is observed. © 2004 American Institute of Physics. [DOI: 10.1063/1.1636264]

## I. INTRODUCTION

The damage produced by ion implantation in crystalline silicon (*c*-Si) substrates is due to atom displacements in the collision cascades. At temperatures above  $\sim 150$  K, the recombination of vacancies and self-interstitials, created by the collision events, is facilitated by the increasing of their mobility. This *in-situ* process, called dynamic annealing, repairs part of the originally produced damage. Since the damage production and the dynamic annealing are competing processes, the final depth distribution of the damage strongly depends on the implantation temperature ( $T_i$ ).<sup>1</sup> Other factors affecting the damage production are the ion mass, energy and dose rate. For temperatures lower than  $\sim 200^\circ\text{C}$ , the damage accumulates preferentially around the maximum energy deposition region. Depending on the ion mass and implanted dose, an amorphous silicon (*a*-Si) layer may develop over there, either buried or extending up to the surface. At higher implantation temperatures ( $T_i > 200^\circ\text{C}$ ), the dynamic annealing process becomes so effective that amorphization of the silicon substrate is blocked.

The *a*-Si layer produced by ion implantation can be recrystallized by solid phase epitaxial growth (SPEG) during furnace annealing at temperatures above  $\sim 450^\circ\text{C}$ .<sup>2</sup> The thermal SPEG process is characterized by a single activation energy of  $\sim 2.7$  eV.<sup>3,4</sup> Besides furnace annealing, SPEG has been observed using different modalities of transient anneal-

ing techniques, like rapid thermal annealing (RTA), pulsed or continuous laser irradiation and electron beam annealing.<sup>4</sup> All these annealing methods use the heating of the material to activate the SPEG process.

A distinct annealing method is the ion beam irradiation of the amorphous material. During ion beam irradiation of *a*-Si clusters embedded in a crystalline substrate at temperatures  $T_i > 100^\circ\text{C}$ , two annealing processes contribute to the recrystallization of the clusters.<sup>5</sup> One of them is the thermal recrystallization process of the isolated amorphous clusters,<sup>6</sup> which can be excited either by an external heat source or by the deposited beam power. The other annealing process is the ion beam induced epitaxial crystallization (IBIEC) produced by the elastic nuclear energy transferred to the atoms in the collision cascades.<sup>7</sup> In the case of a continuous *a*-Si layer irradiated with ions at temperatures  $T_i < 450^\circ\text{C}$ , the recrystallization process is activated exclusively by the deposited ion energy, since the thermal SPEG rate of the *a*-Si layer is negligible in this temperature range. The IBIEC rate is influenced by the presence of impurity atoms in the *a*-Si layer, in a likewise manner to that of thermal SPEG.<sup>8–10</sup> Hence, dopant atoms, like B, P and As, enhances the IBIEC rate<sup>7</sup> whereas O atoms reduces it.<sup>7,11,12</sup> For ion implantation at temperatures  $T_i < 200^\circ\text{C}$ , the damage accumulation prevails over the IBIEC process, leading to the expansion of the existing *a*-Si region through layer by layer amorphization.

The IBIEC phenomenon has been observed during ion implantation performed at high dose rates, if the sample temperature is allowed to raise progressively by the beam power.<sup>13</sup> At the beginning of the process, while the temperature is below  $200^\circ\text{C}$ , a buried *a*-Si layer may be formed.

<sup>a)</sup>Present address: IBM Thomas J. Watson Research Center, P.O. Box 218, 10598, Yorktown Heights, New York.

<sup>b)</sup>Electronic mail: carlos-cima@sct.rs.gov.br

With further accumulation of the dose, the sample temperature may surpass 200 °C. Then, the IBIEC of the *a*-Si layer takes place, eventually leaving the material single crystalline. Ridgway *et al.*<sup>14</sup> demonstrated that the IBIEC phenomenon can also occur during a low dose rate implant. The authors observed the recrystallization of an original *a*-Si layer induced by O<sup>+</sup> implantation carried out at temperatures of 200 °C and 245 °C.

In order to clearly observe the IBIEC phenomenon, most of the experiments reported in the scientific papers have been performed using an ion beam traversing a continuous or a buried *a*-Si layer, at temperatures in the range 200 °C <  $T_i$  < 400 °C.<sup>7</sup> The measured activation energies for the IBIEC process varies from 0.18 eV to 0.38 eV.<sup>7,15,16</sup>

In the present study we consider the case where three sequential O<sup>+</sup> implants, realized at the same energy, were accumulated in the samples. The first implant was performed at an elevated temperature, to maintain the material single crystalline, with a dose sufficiently high to establish a peak oxygen atom concentration of ~3 at.% near the surface. This was followed by a RT implantation aimed to create a buried *a*-Si layer. The third implant conducted on the samples employed different substrate temperatures to modify the thickness of the original *a*-Si layer, either by ion beam induced amorphization or ion beam induced recrystallization. The contribution of the thermal SPEG to the recrystallization process can be disregarded in these samples, since its rate is negligible in *a*-Si layers containing high oxygen atom concentrations, even for temperatures above 550 °C.<sup>17</sup> The structure of the residual defects in the recrystallized material and the IBIEC rate at different temperatures were investigated. The results of the present study could be applied to the understanding of the defects formed by oxygen implantation of silicon, when the sample temperature varies during the implantation process. In particular, the defect structures in O<sup>+</sup> implanted silicon play a significant role in the synthesis of silicon on insulator (SOI) substrates prepared by the method of separation by implanted oxygen (SIMOX).

## II. EXPERIMENTAL DETAIL

Czochralski-grown (100) silicon wafers of *p*-type conductivity, with resistivity of 8–12 Ω cm, were implanted with <sup>16</sup>O<sup>+</sup> ions at a fixed energy of 185 keV. According to TRIM<sup>18</sup> code simulation, the mean projected range ( $R_p$ ) and standard deviation ( $\Delta R_p$ ) of these implants are 375 nm and 84 nm, respectively. After cleaning, the wafers were implanted at 600 °C to a dose of  $5 \times 10^{16}$  cm<sup>-2</sup>. Subsequently, a nominal room temperature (RT) implantation to the dose of  $4 \times 10^{15}$  cm<sup>-2</sup> was performed with the purpose of creating a buried amorphous layer. A set of samples was then submitted to oxygen implantation in the temperature range of 150–600 °C, with doses varying from  $2 \times 10^{16}$  to  $8 \times 10^{16}$  cm<sup>-2</sup>. All the implants were conducted limiting the beam current density to the range of 1–3 μA cm<sup>-2</sup>. In order to minimize channeling effects, the sample normal was tilted by 7° in respect to the beam incidence direction and twisted 25° in respect to the <110> planar direction. During the implants, the samples were held on a graphite plate by metallic

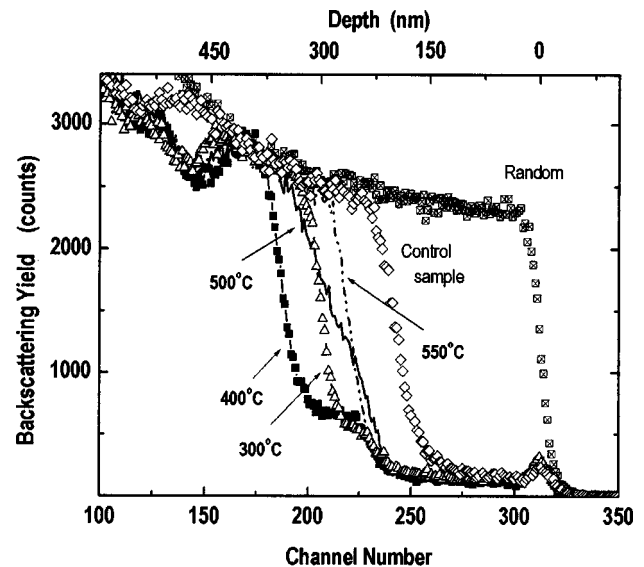


FIG. 1. Random and aligned RBS spectra of oxygen implanted silicon sample ( $5 \times 10^{16}$  cm<sup>-2</sup>/600 °C, followed by  $4 \times 10^{15}$  cm<sup>-2</sup>/RT) before (“Control sample”) and after an additional implantation to the dose of  $5 \times 10^{16}$  cm<sup>-2</sup> at the temperatures of 300 °C, 400 °C, 500 °C and 550 °C.

clamps. A halogen lamp installed on the backside of the plate provided a source of heat to maintain the temperature constant while the sample was being irradiated. The temperature was monitored and controlled by a proportional-integral-derivative (PID) controller through a bonded thermocouple, ensuring a maximum deviation of  $\pm 2$  °C from the set-point.

The samples were analyzed by Rutherford Backscattering Spectrometry (RBS) employing a 900 keV He<sup>+</sup> beam in the random or aligned direction. Additionally, some selected samples were observed by cross section transmission electron microscopy (TEM) using a JEM 2010 microscope operating at 200 kV.

## III. RESULTS AND DISCUSSION

Figure 1 presents the RBS spectra of samples submitted to IBIEC induced by a high temperature oxygen implantation performed to a fixed dose of  $5 \times 10^{16}$  cm<sup>-2</sup>. The spectrum corresponding to the original amorphous layer created by the double implantation procedure described in the previous section is labeled as a “Control sample.” The thickness of the *a*-Si layer is approximately 300 nm. In accordance with previous studies,<sup>19,20</sup> the near surface region (until the depth of ~150 nm in the present case) is apparently defect free after a high temperature implantation. In fact, this region accumulates a high density of vacancy clusters as a result of the ion implantation conditions, leading to the appearance of a localized mechanical strain in the crystal lattice.

One can easily notice that, in the range from 300 °C to 400 °C, the IBIEC progressed with the temperature. There is a small plateau in the spectrum corresponding to the 400 °C implant, indicating the presence of a defect distribution in the recrystallized material. It starts at a depth of ~220 nm and ends at ~330 nm, followed by a ~100 nm thick *a*-Si layer, marked by the random level of its backscattering yield.

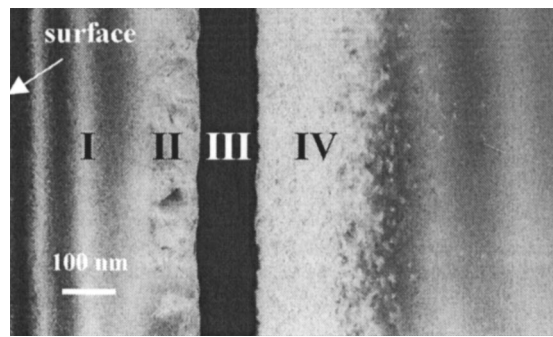


FIG. 2. Cross section TEM image of sample submitted to IBIEC at 400 °C (corresponds to the spectrum labeled “400 °C” in Fig. 1).

For implantation temperatures higher than 400 °C (500 °C and 550 °C), the IBIEC phenomenon is remarkably less effective.

Figure 2 shows the cross section TEM photomicrograph of the sample after IBIEC at 400 °C (corresponding to the spectrum labeled “400 °C” in Fig. 1). A defect structure composed by four layers (labeled as I, II, III and IV) is disclosed in this figure. Layer I is apparently defect free and extends from the surface up to the depth of 220 nm. Layer II consists of an ~100 nm thick single crystalline layer containing an array of microtwins, as evidenced by the correlation between the twin particles dark field images with specific extra spots on the selected area diffraction patterns along the  $\langle 110 \rangle$  zone axis. These residual defects are responsible for the small plateau in the corresponding aligned RBS spectrum in Fig. 1. Layer III is a ~100 nm thick *a*-Si layer. Layer IV is a ~180 nm thick *c*-Si layer displaying a dense dislocation network and microtwins. The microtwins in layers II and IV results from the IBIEC of *a*-Si material with a high oxygen atom concentration (up to ~7 at. %). This complies with the observation, by Spinella *et al.*,<sup>12</sup> of twinning in ion beam recrystallized *a*-Si layers deposited on *c*-Si substrates, when the interface between these two materials is contaminated with oxygen atoms.

In a separate experiment, a silicon sample were submitted to IBIEC at 400 °C in identical conditions of those of the sample analyzed in Fig. 2, except by the third oxygen dose, which was increased to  $8 \times 10^{16} \text{ cm}^{-2}$ . Despite the fact that the oxygen atom concentration reaches ~8 at. % at its peak, the entire *a*-Si layer was recrystallized. The TEM image of this sample (not shown) revealed a layered defect structure likewise the one shown in Fig. 2, however, with the *a*-Si layer (Layer III in Fig. 2) replaced by a heavily damaged *c*-Si one.

The aligned RBS spectrum of the sample implanted at 500 °C (see Fig. 1) differs significantly from those implanted at 300 or 400 °C. A structure composed by three layers is observed. The first layer extends from the surface up to the depth of 220 nm. Within the sensitivity of the RBS analysis, no residual defects are noticed in this near surface layer. The second layer, extending from 220 to 420 nm, has preserved its crystalline nature, since the corresponding backscattering yield is below the random level. However, this layer contains a residual defect distribution, as shown by the progressive

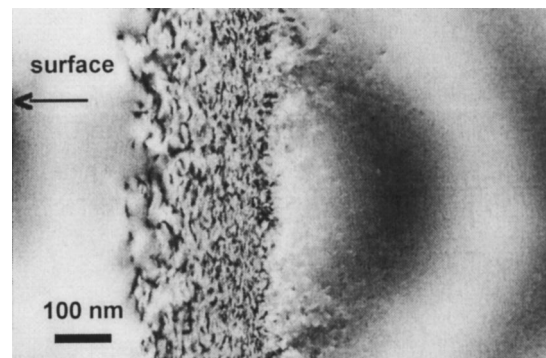


FIG. 3. Cross section TEM image of sample submitted to IBIEC at 550 °C (corresponds to the spectrum labeled “550 °C” in Fig. 1).

increase of its backscattering yield towards the random level. Immediately below, there is a 70 nm amorphous layer (showing random level backscattering counts). Rising the third implantation temperature to 550 °C, an abrupt interface develops at the depth of 250 nm, separating a defect free near surface layer and a highly defective one (170 nm thick). The backscattering yield from the latter layer coincides with the random level. Identical results were obtained in a sample implanted at 600 °C (the spectrum not shown).

The cross section TEM micrograph from observations of a sample corresponding to the spectrum labeled “550 °C” in Fig. 1 is depicted in Fig. 3. In close agreement with the RBS data, the implanted material presents a double layer structure. In the near surface layer, extending up to the depth of ~250 nm, no residual defects are observed in the TEM image. The next layer, comprising the depths from 250 to 450 nm, consists of a highly damaged crystalline material and a distribution of small  $\text{SiO}_x$  precipitates. This buried defect band correlates with the backscattering yield at the random level (see the spectrum for a 550 °C implant in Fig. 1).

As was mentioned above, two different regimes of IBIEC can be distinguished. At implantation temperatures of 300 °C and 400 °C the recrystallized layer is single crystal silicon with a high concentration of extended defects. Continuing the IBIEC up to the dose of  $8 \times 10^{16} \text{ cm}^{-2}$  at temperature of 400 °C we succeeded full recrystallization of the amorphous layer. Hence, one can conclude that, for these temperatures, the IBIEC moving front preserves complete lattice periodicity in the crystalline side of the interface, without forming grain boundaries. The second range of temperatures (500 °C–600 °C) favors the nucleation of small  $\text{SiO}_x$  precipitates in the amorphous layer, drastically increasing the concentration of extended defects during IBIEC (to a level which correlates with random backscattering yield in the RBS spectrum). Observing Fig. 1 for these temperatures, it could be suggested that this layer is polycrystalline, but TEM diffraction patterns show a highly defective single crystalline layer (see Fig. 3).

The influence of  $\text{O}^+$  implant temperature on the IBIEC process was also investigated using the dose of  $2 \times 10^{16} \text{ cm}^{-2}$  for the third oxygen implantation. The temperature, in this case, varied from 100 to 400 °C. The implantation performed at 100 °C expanded the *a*-Si layer thickness as a consequence of a layer by layer amorphization process.

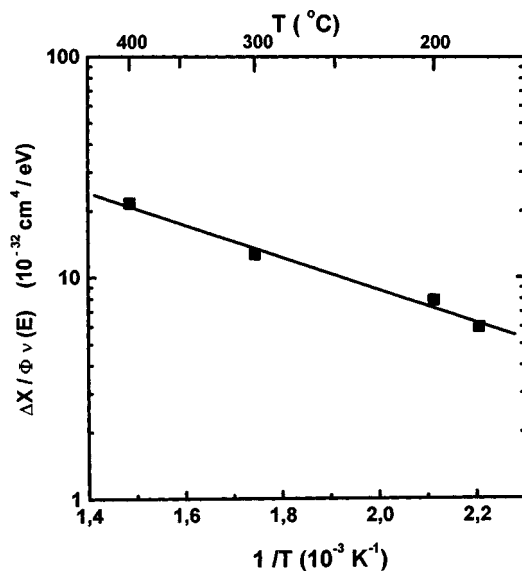


FIG. 4. Arrhenius plot of the implantation induced epitaxial growth at the front amorphous–crystalline interface of a buried amorphous layer. The samples received the third implant with a fixed dose of  $2 \times 10^{16} \text{ cm}^{-2}$ , but at distinct temperatures.

At 150 °C, a balance between amorphization and IBIEC occurred, leaving the thickness of the amorphous layer unaltered, in agreement with previously published results.<sup>5</sup> Above 150 °C, the third implantation reduced progressively the thickness of the *a*-Si layer as the temperature increased.

In Fig. 4, the extent of the epitaxial growth of the front *a*-*c* interface, normalized by the dose and deposited beam energy at this interface, is plotted against the reciprocal of the absolute temperature of the third implantation. The points of this graph were calculated from the data produced in the experiment with the IBIEC temperature varying from 150 to 400 °C. In the expression for the normalized growth,  $\Delta X$  is the depth of the regrowth layer in the front *a*-*c* interface,  $\Phi$  is the ion dose of the third implant ( $2 \times 10^{16} \text{ cm}^{-2}$ ) and  $\nu(E)$ , the energy deposited by atom displacements at the front *a*-*c* interface as estimated by TRIM<sup>18</sup> code simulation. The points in Fig. 4 are well fitted by a linear relationship, from which an apparent activation energy of 0.14 eV  $\pm$  0.05 eV is obtained. This value is inferior to the activation energy of 0.23 eV obtained by Kinomura *et al.*<sup>15</sup> for the IBIEC process stimulated by high energy O<sup>+</sup> beam irradiation at temperatures below 275 °C. However, in the present study, the O<sup>+</sup> beam helps the recrystallization of an *a*-Si layer where the oxygen atom concentration is in the range of 2–4 at.%. The lower apparent activation energy in our investigation indicates that the oxygen atom contamination in the *a*-Si layer decreases the thermal dependence of the IBIEC process. Very likely, the interaction between the ion beam and the point defects at or nearby the *a*-*c* interface affects the diffusion of the latter ones in the *c*-Si containing a high oxygen atom concentration.

#### IV. CONCLUSION

The effects introduced in a buried *a*-Si layer by elevated temperature O<sup>+</sup> implantation were investigated. It was found

that for implantation temperatures lower than 150 °C, the *a*-Si layer expands via layer by layer amorphization of the front and back *a*-*c* interfaces. At temperatures above 150 °C, the implantation stimulates the epitaxial recrystallization of the *a*-Si layer. The recrystallized material presents defect structures differentiated according to the implantation temperature. For implants carried out at 400 °C, the IBIEC leaves an array of microtwins, where the oxygen atom concentration was in the range of 1–3 at.% and a dislocation band for higher oxygen concentrations. At 550 °C, the recrystallized layer contains only a buried dislocation band and small SiO<sub>x</sub> precipitates, distributed over the end of range of the implanted atoms, where the oxygen atom concentration is above 2 at.%. The rate of ion induced epitaxial growth was measured in the temperature range of 180–400 °C. A straight linear relationship fitted all the data points in an Arrhenius plot, from which an apparent activation energy of 0.14 eV  $\pm$  0.05 eV was obtained. This activation energy is lower than the ones previously published for the IBIEC process. This lower value indicates lower temperature dependence for the IBIEC process in the presence of a high oxygen atom concentration.

#### ACKNOWLEDGMENTS

This work was partially supported by Conselho Nacional de Desenvolvimento Científico e Tecnológico (CNPq) and Fundação de Amparo à Pesquisa do Estado do Rio Grande do Sul (FAPERGS).

- <sup>1</sup>J. P. de Souza and D. K. Sadana, in *Handbook on Semiconductors*, edited by S. Mahajan (North-Holland, Amsterdam, 1994), Vol. 3B, p. 2036.
- <sup>2</sup>L. Csepregi, J. W. Mayer, and T. W. Sigmon, *Phys. Lett. A* **54**, 157 (1975).
- <sup>3</sup>S. A. Kokorowski, G. L. Olson, and L. D. Hess, *J. Appl. Phys.* **53**, 921 (1982).
- <sup>4</sup>G. L. Olson and J. A. Roth, *Mater. Sci. Rep.* **3**, 1 (1988).
- <sup>5</sup>B. Zeroal and G. Carter, *Nucl. Instrum. Methods Phys. Res. B* **44**, 318 (1990).
- <sup>6</sup>R. S. Nelson, in *Proceedings of the European Conference on Ion Implantation* (Peter Peregrinus, Stevenage, 1970, England), p. 212.
- <sup>7</sup>F. Priolo and E. Rimini, *Mater. Sci. Rep.* **5**, 319 (1990).
- <sup>8</sup>J. S. Williams and R. G. Elliman, *Appl. Phys. Lett.* **37**, 829 (1980).
- <sup>9</sup>L. Csepregi, E. F. Kennedy, T. J. Gallagher, J. W. Mayer, and T. W. Sigmon, *J. Appl. Phys.* **48**, 4234 (1977).
- <sup>10</sup>E. F. Kennedy, L. Csepregi, J. W. Mayer, and T. W. Sigmon, *J. Appl. Phys.* **48**, 4241 (1977).
- <sup>11</sup>F. Priolo, C. Spinella, A. La Ferla, A. Battaglia, E. Rimini, G. Ferla, A. Carnera, and A. Gasparotto, *Mat. Res. Soc. Symp. Proc.* **128**, 563 (1989).
- <sup>12</sup>C. Spinella, F. Priolo, E. Rimini, and G. Ferla, *Nuovo Cimento D* **11**, 1805 (1989).
- <sup>13</sup>S. Cannavò, M. G. Grimaldi, E. Rimini, G. Ferla, and L. Gandolfi, *Appl. Phys. Lett.* **47**, 138 (1985).
- <sup>14</sup>M. C. Ridgway, R. Locciano, J. S. Williams, A. P. Pogany, and D. K. Sengupta, *Mat. Lett.* **10**, 156 (1990).
- <sup>15</sup>A. Kinomura, A. Chayahara, N. Tsubouchi, Y. Horino, and J. S. Williams, *Nucl. Instrum. Methods Phys. Res. B* **148**, 370 (1999).
- <sup>16</sup>J. S. Williams, R. G. Elliman, W. L. Brown, and T. E. Seidel, *Phys. Rev. Lett.* **55**, 1482 (1985).
- <sup>17</sup>E. F. Kennedy, L. Csepregi, J. W. Mayer, and T. W. Sigmon, *J. Appl. Phys.* **48**, 4241 (1977).
- <sup>18</sup>J. F. Ziegler, J. P. Biersack, and U. Littmark, in *The Stopping and Range of Ions in Solids* (Pergamon, Oxford, 1985), Vol. 1.
- <sup>19</sup>J. P. de Souza, Yu. Suprun-Belovich, H. Boudinov, and C. A. Cima, *J. Appl. Phys.* **87**, 8385 (2000).
- <sup>20</sup>J. P. De Souza, Yu. Suprun-Belovich, H. Boudinov, and C. A. Cima, *J. Appl. Phys.* **89**, 42 (2001).